OMTON, Volume *32*

Supplemental information

Targeting the membrane-proximal C2-set domain of CD33 for improved CAR T cell therapy

Salvatore Fiorenza, Sheryl Y.T. Lim, George S. Laszlo, Erik L. Kimble, Tinh-Doan Phi, Margaret C. Lunn-Halbert, Delaney R. Kirchmeier, Jenny Huo, Hans-Peter Kiem, Cameron J. Turtle, and Roland B. Walter

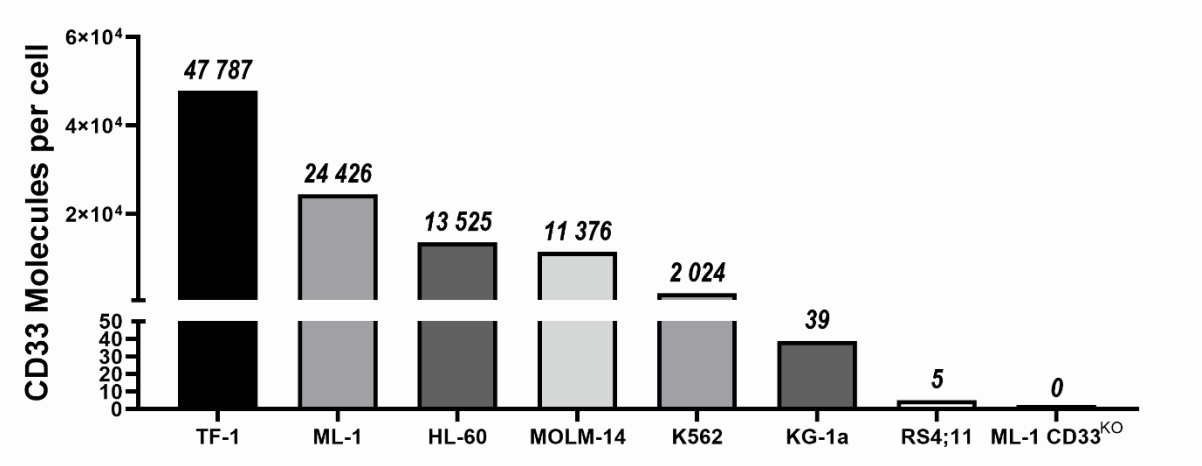

Figure S1.

CD33 molecules expressed on the surface of cell lines. Number of CD33 surface molecules as quantitated by flow cytometry using Quantibrite-PE.

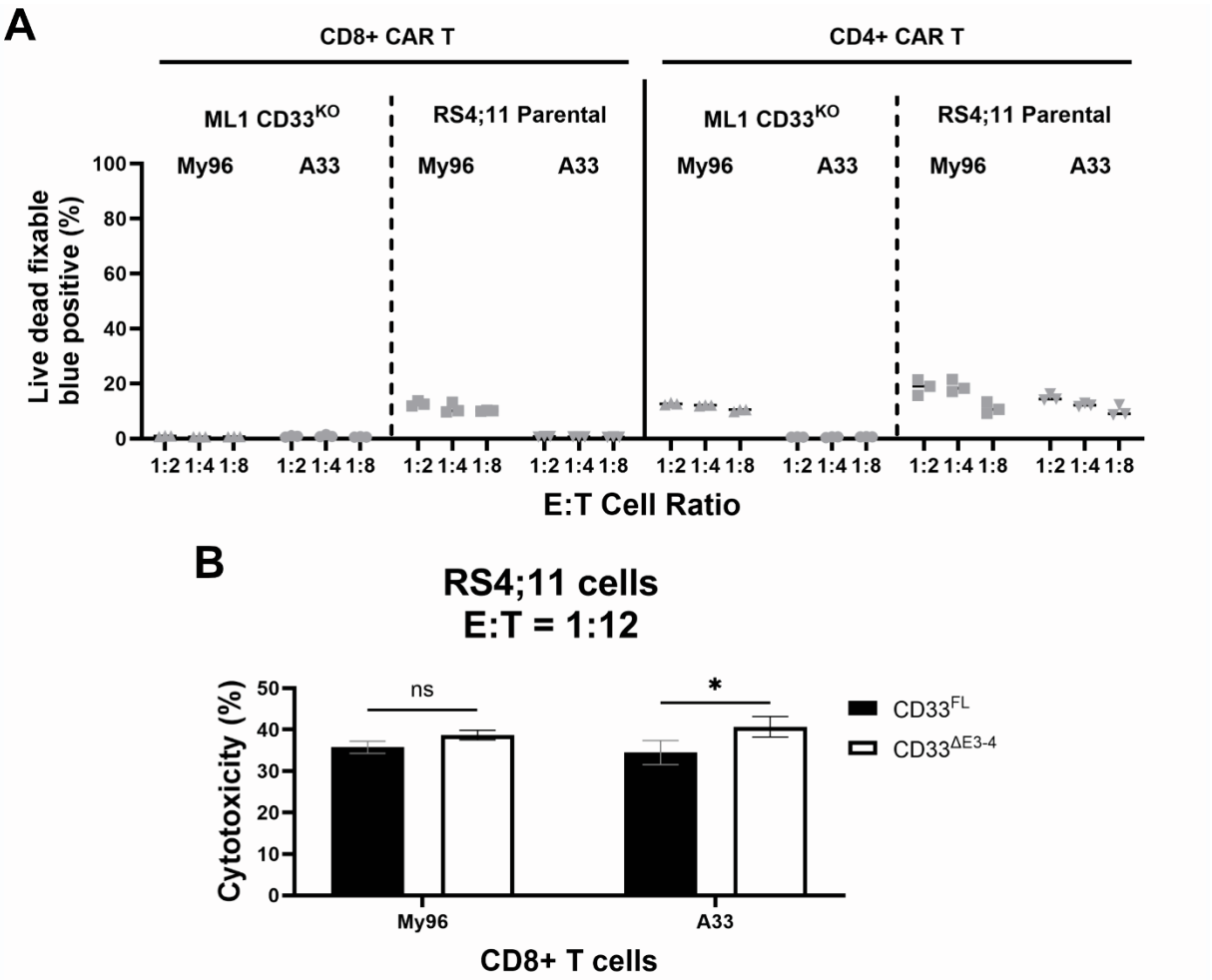

Figure S2.

Cytotoxicity of CD33$^{V\text{-}set}$ CAR T cells against RS4;11 cells at low antigen expression and low E:T. (A) Percent positive live dead fixable blue (DAPI) cell parental RS4;11 or ML-1 CD33^{KO} when co-cultured with primary human CD8^{+} T cells expressing either an My96-based CAR construct or an A33-based CAR construct for 16 hours. Shown are raw individual data points from triplicate experiments. **(B)** Primary human CD8^{+} T cells expressing either an My96-based CAR construct or an A33-based CAR construct were incubated with parental RS4;11 cells or RS4;11 cells transduced with either CD33^{FL} or CD33$^{\Delta E3\text{-}4}$ at an effector to target (E:T) cell ratio of 1:12 for 16 hours before flow cytometric assessment of cytotoxicity. Shown are mean ± SD of % cytotoxicity relative to parental RS4;11 cells. *P<0.05, ns (not significant) by two-way ANOVA with post-hoc Tukey correction. Shown are technical triplicates of one representative experiment.

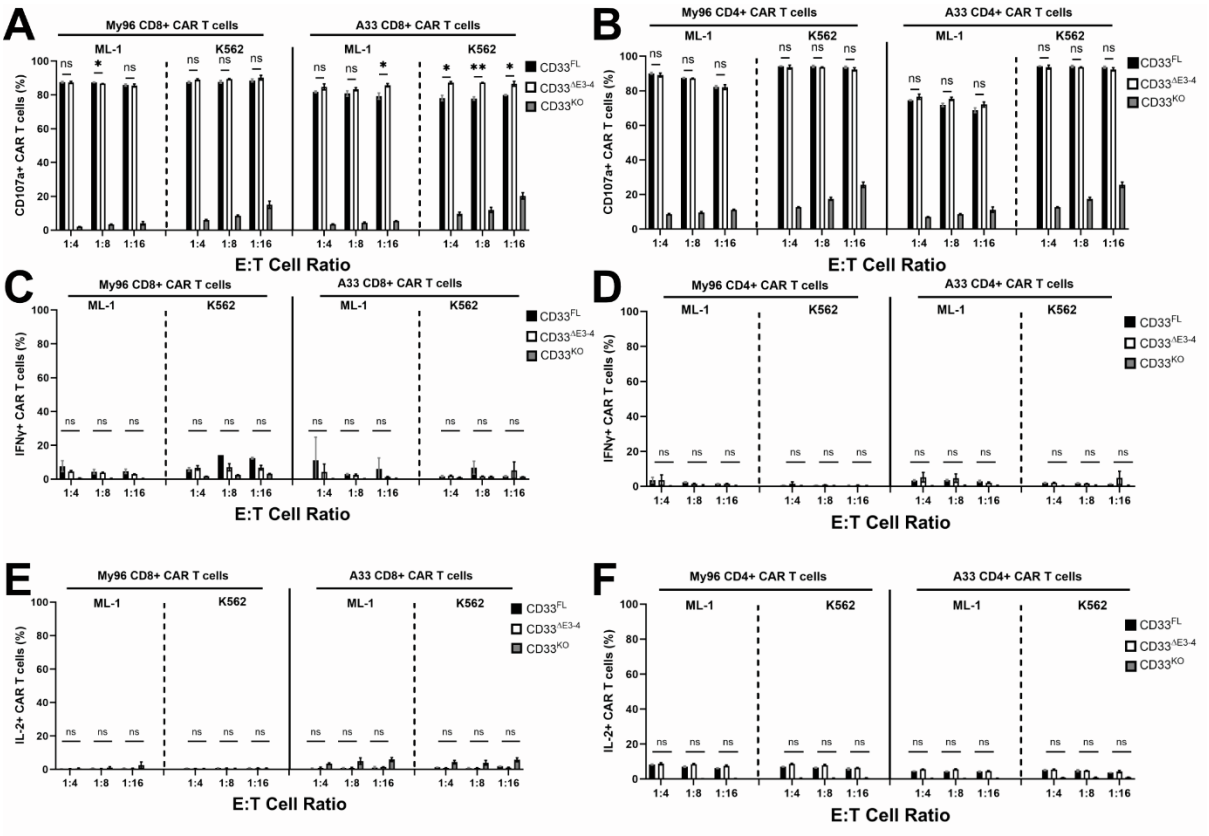

Figure S3.

Degranulation marker and intracellular cytokine production with shorter membrane-membrane distance. (A-B) CD107a, and **(C-F)** intracellular cytokine staining by multiparameter flow cytometry in **(A, C, E)** CD8+ and **(B, D, F)** CD4+ CD33$^{V\text{-}set}$ My96 or A33 CAR T cells following 12-20 hours co-culture with ML-1 or K562 cells with CRISPR/Cas9-mediated deletion of the endogenous CD33 locus (C33^{KO}) or sublines engineered to overexpress full length CD33 (FL) or CD33 without the C2-set domain (CD33$^{\Delta E3\text{-}4}$) via lentiviral gene transfer at various effector to target (E:T) cell ratios as indicated. Shown are mean ± SD in triplicate from two representative experiments. *P<0.05, **P<0.01, ns (not significant) by two-way ANOVA with post-hoc Tukey correction.

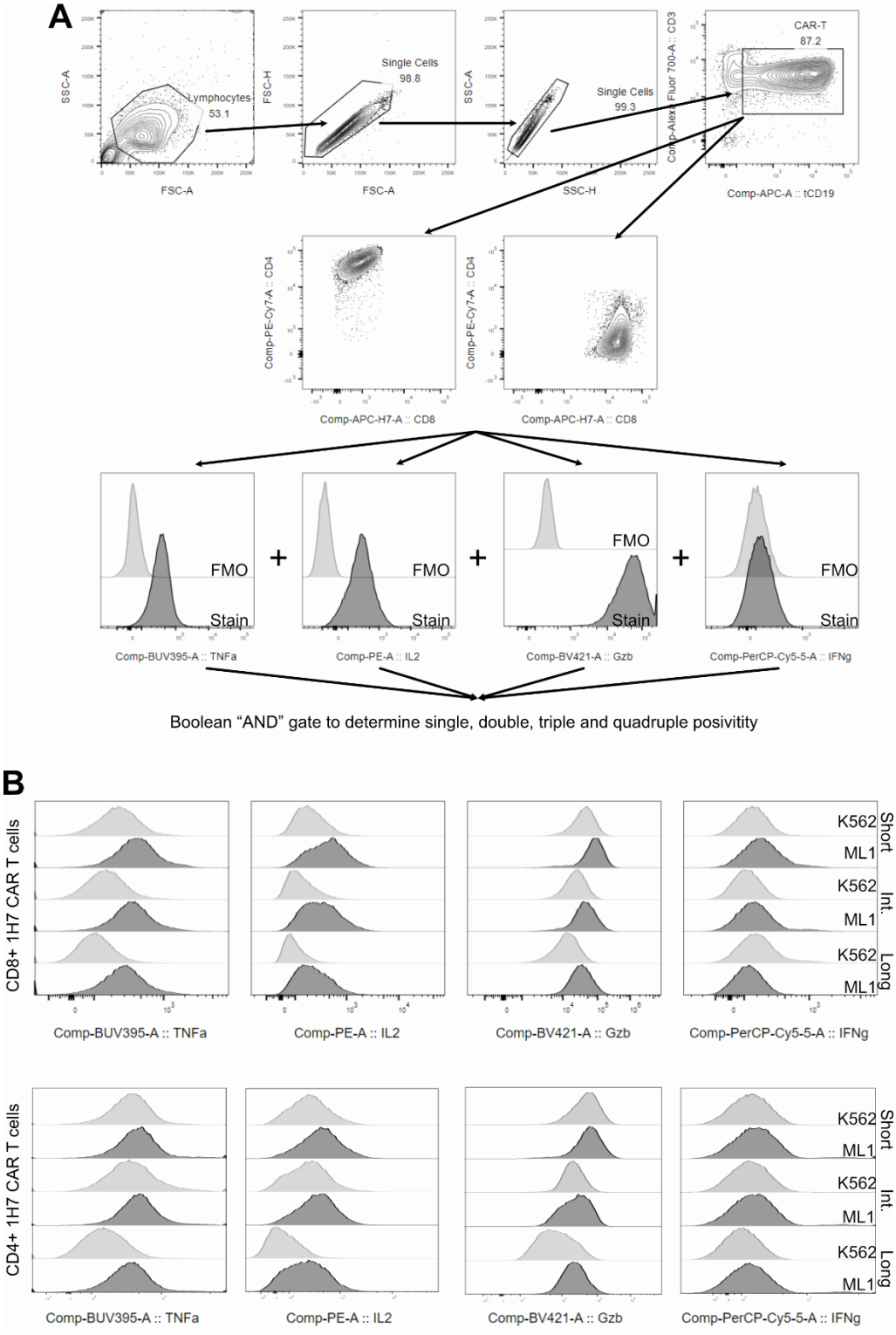

Figure S4.

Flow cytometric analysis of intracellular cytokine expression. (A) Gating strategy for assessment of polyfunctionality. **(B)** Representative flow cytometry histogram plots of intracellular cytokine expression in CD8+ and CD4+ 1H7 CAR T cells with varying spacer lengths co-cultured with K562 and ML-1 AML cells.

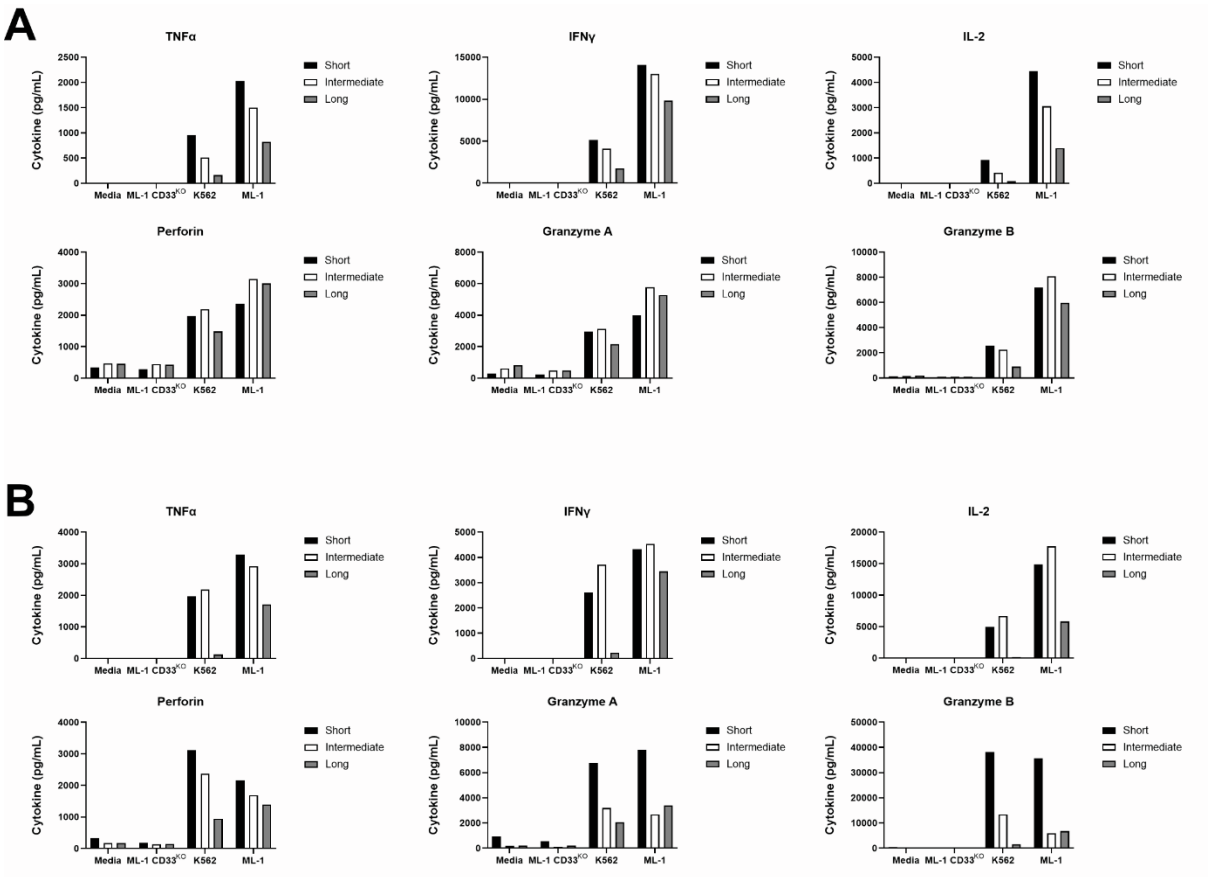

Figure S5.

Effect of spacer length on CAR T cell-induced production of cytokines, perforin, granzyme A, and granzyme B. Cytokine secretion following 24-hour co-culture of AML cell lines with **(A)** CD8+ CD33^{PAN} 1H7 CAR T cells and **(B)** CD4+ CD33^{PAN} 1H7 CAR T cells with different spacer lengths. Shown are mean cytokine concentration in duplicate.

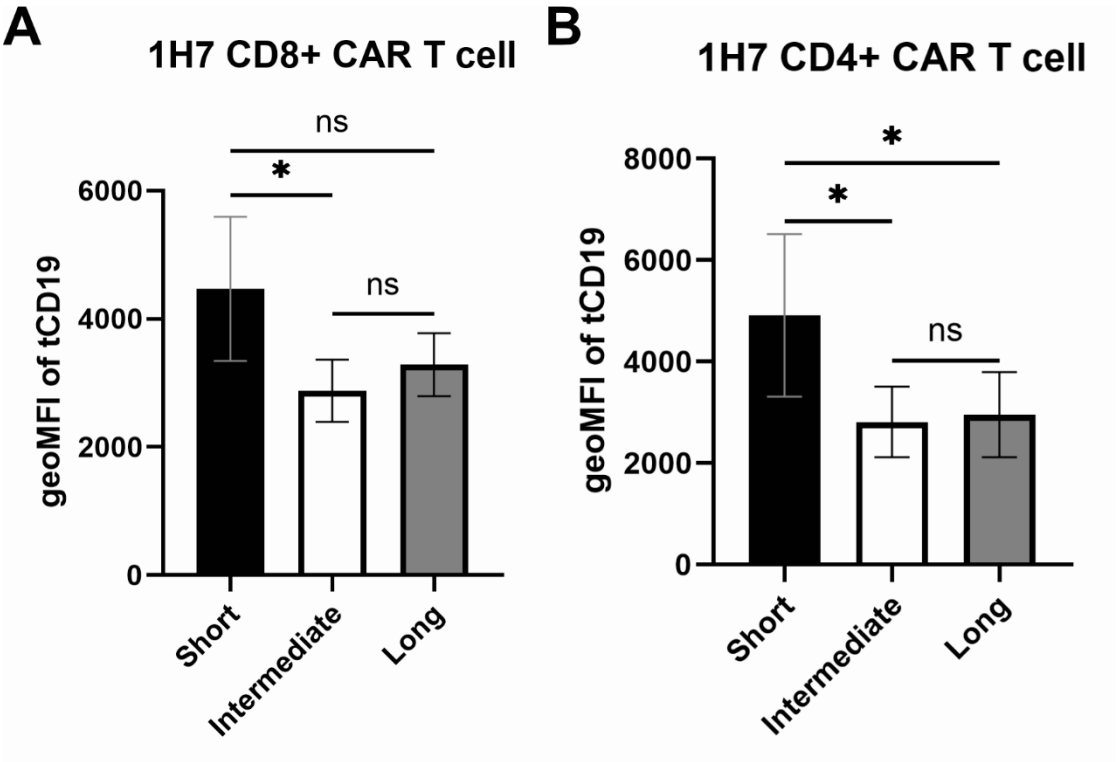

Figure S6.

Transgene expression of surface transduction marker molecules (tCD19) on 1H7 CD33^{PAN} (A) CD8+ and (B) CD4+ CAR T cells. Shown are mean ± SD values from technical triplicates. *P<0.05, ns (not significant) by two-way ANOVA with post-hoc Tukey correction.

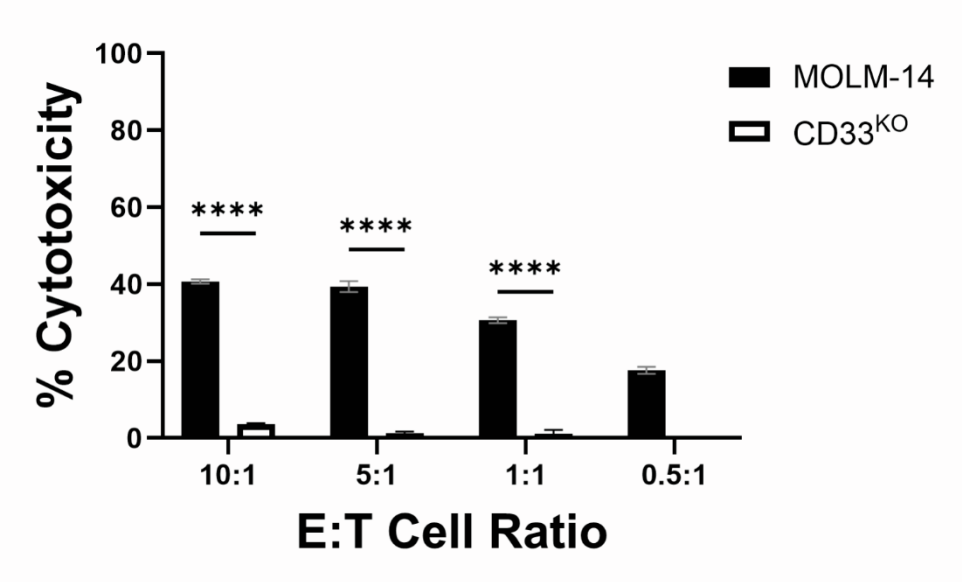

Figure S7.

Cytotoxicity of 1H7 CAR T cells following co-culture with parental MOLM-14 or CD33^{KO} cells. Primary human CD8^{+} T cells 1HY.int CAR construct were incubated with chromium^{51}-labelled parental MOLM-14 cells or CD33^{KO} at decreasing effector to target (E:T) cell ratios for four fours. Chromium within supernatant was then assessed by scintillation counting and calculated as per Materials and Methods. Shown are mean ± SD of calculated % cytotoxicity. ****P<0.0001, by two-way ANOVA with post-hoc Tukey correction. Shown are technical triplicates of one representative experiment.

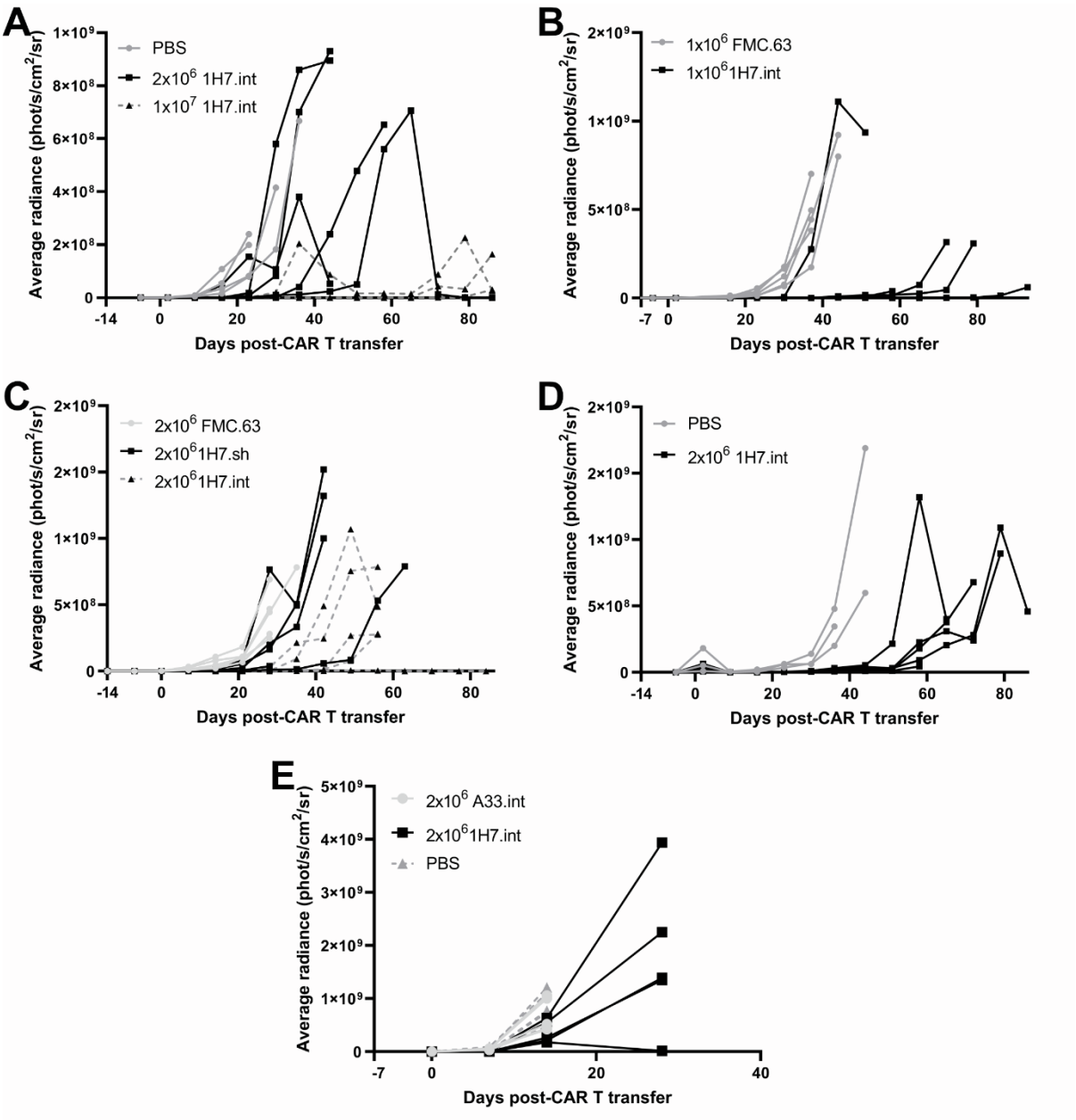

Figure S8.

Bioluminescence of NSG mice bearing human AML cell line derived xenografts.

Immunodeficient NSG mice were injected with GFP-expressing $2x10^6$ HL-60 **(A)**, $1x10^6$ HL-60 **(B)**, $2x10^6$ HL-60 **(C)**, $2x10^6$ KG-1a **(D)** or $5x10^5$ MOLM-14 cells **(E)**. Two weeks **(A,C** and **D)** or one week **(B** and **E)** later, mice received either 1H7 $CD33^{PAN}$ CAR T cells with an intermediate (int) or short (sh) spacer (n=5), A33 CAR T cells (n=5) or CD19-directed CAR T (FMC63, n=5) in a 1:1 ratio of CD4:CD8 T cells or were given vehicle control (PBS, n=4 for HL-60, n=3 for KG-1a, n=5 for MOLM-14). Mice were monitored weekly for bioluminescence by anaesthetization and intraperitoneal injection of luciferin followed by imaging. Note: that if animals were deemed too unwell for anaesthetization they were not imaged.

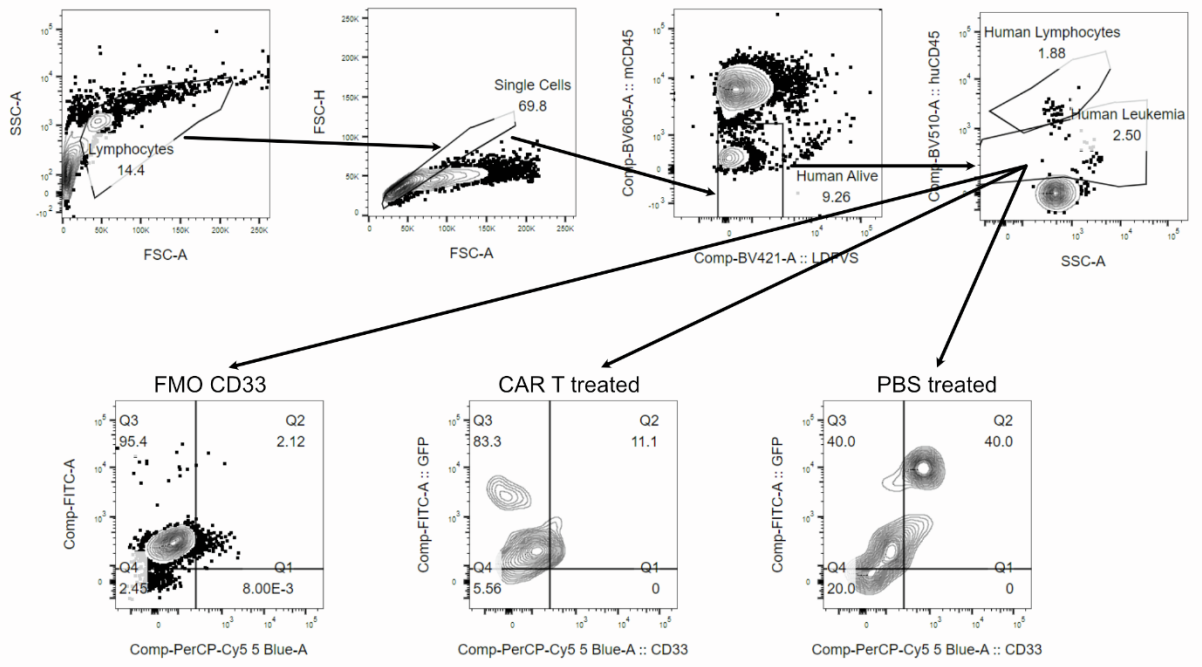

Figure S9.

Gating strategy to identify CD33+ and CD33- cells in cells engrafted with human KG-1a cells. Representative flow cytometry plot of gating of non-mouse cells by exclusion of mouse CD45+ cells, with human lymphocytes and human leukemia identified by expression of human CD45. Three representative plots from FMO stained and PBS-treated, CAR T-treated and PBS-treated mice to show gating of GFP versus CD33.

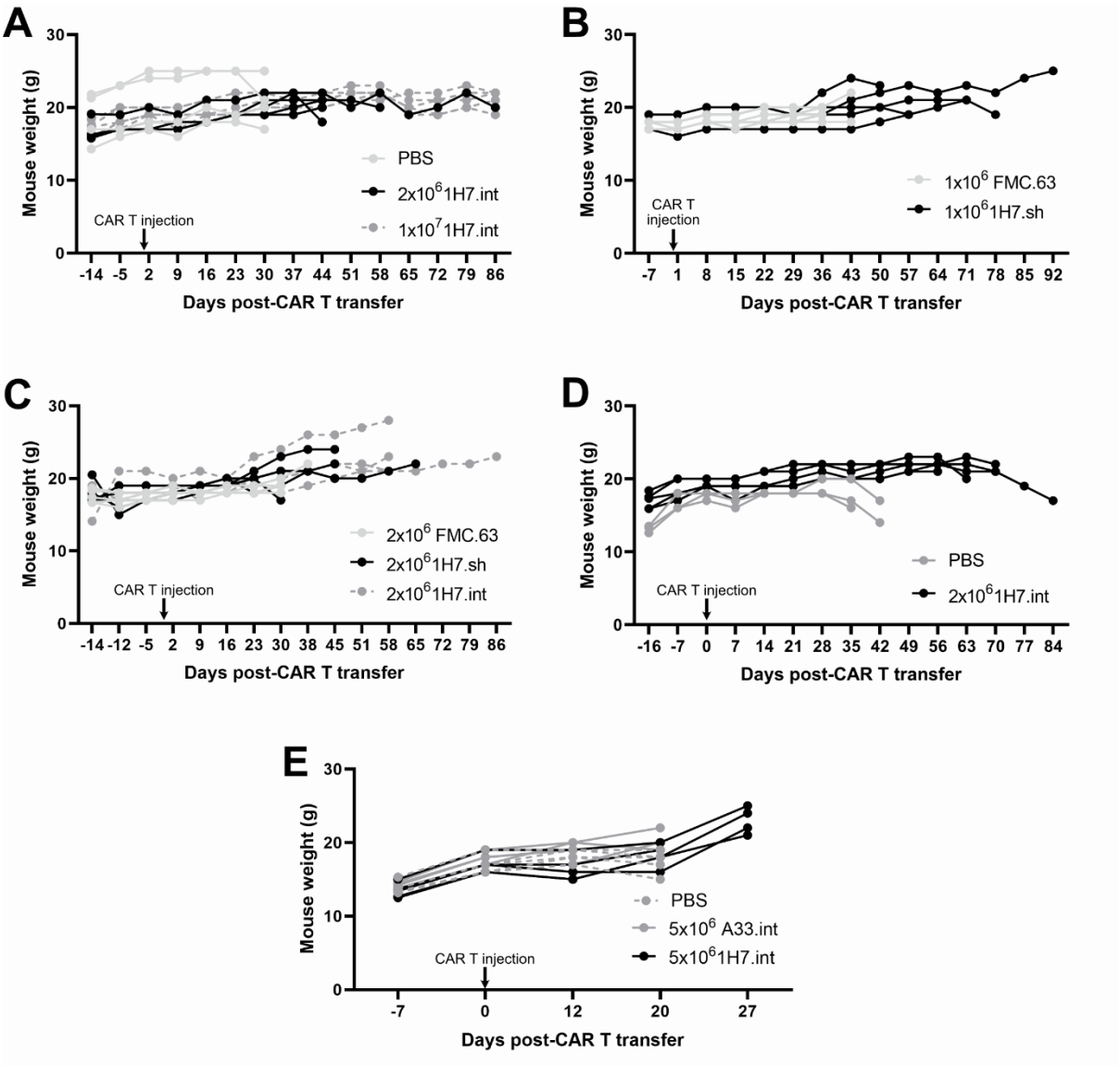

Figure S10.

Individual weights of mice bearing human AML cell line derived xenografts following treatment with 1H7 CAR T cells, A33 CAR T cells, control FMC.63 (CD19) CAR T cells, or PBS. Immunodeficient NSG mice were injected with GFP-expressing $2x10^6$ HL-60 **(A)**, $1x10^6$ HL-60 **(B)**, $2x10^6$ HL-60 **(C)**, $2x10^6$ KG-1a **(D)** or $5x10^5$ MOLM-14 cells **(E)**. Two weeks **(A,C** and **D)** or one week **(B** and **E)** later, mice received either 1H7 $CD33^{PAN}$ CAR T cells with an intermediate (int) or short (sh) spacer (n=5), A33 CAR T cells (n=5) or CD19-directed CAR T (FMC63, n=5) in a 1:1 ratio of CD4:CD8 T cells or were given vehicle control (PBS, n=4 for HL-60, n=3 for KG-1a, n=5 for MOLM-14). Mice were monitored weekly for weight. Note: animals that were deemed unwell were weighed more regularly.

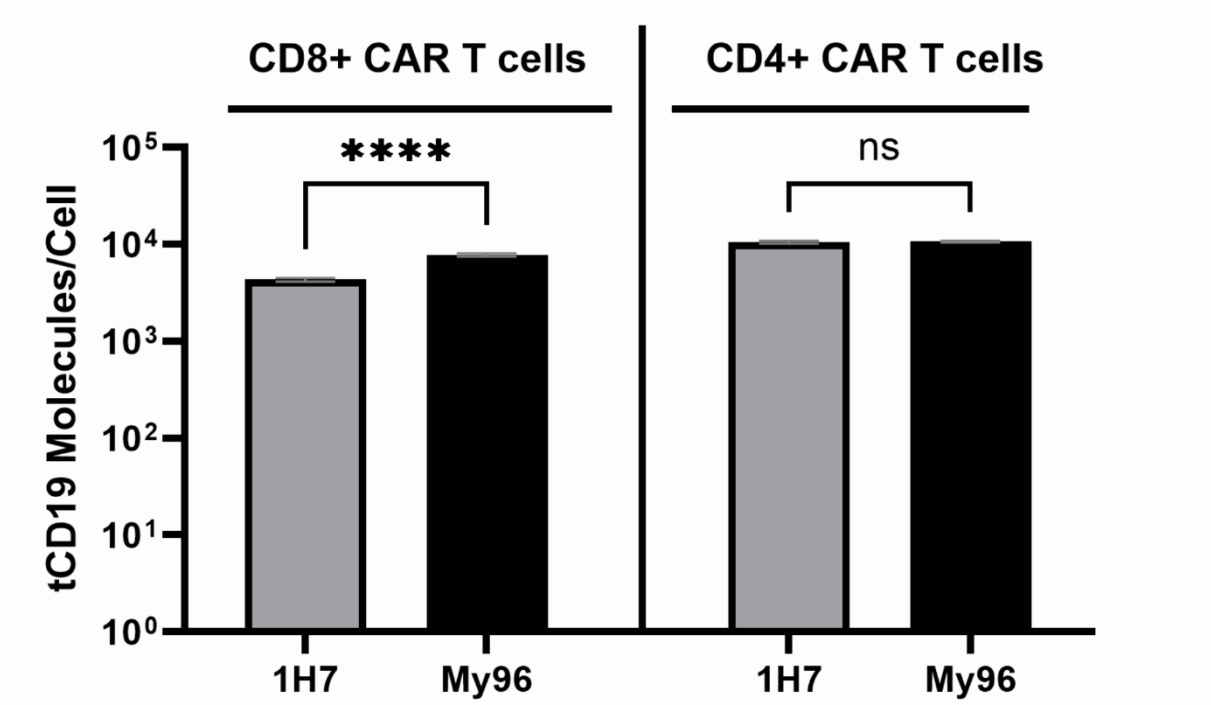

Figure S11.

Expression of the CAR transduction marker, truncated CD19 (tCD19), on My96 and 1H7 CAR T cells. Expression of tCD19 molecules was assessed by Quantibrite-PE analysis on CD8+ and CD4+ CAR T cells. ****P<0.0001, ns (not significant) by one-way ANOVA analysis with post-hoc Tukey test.

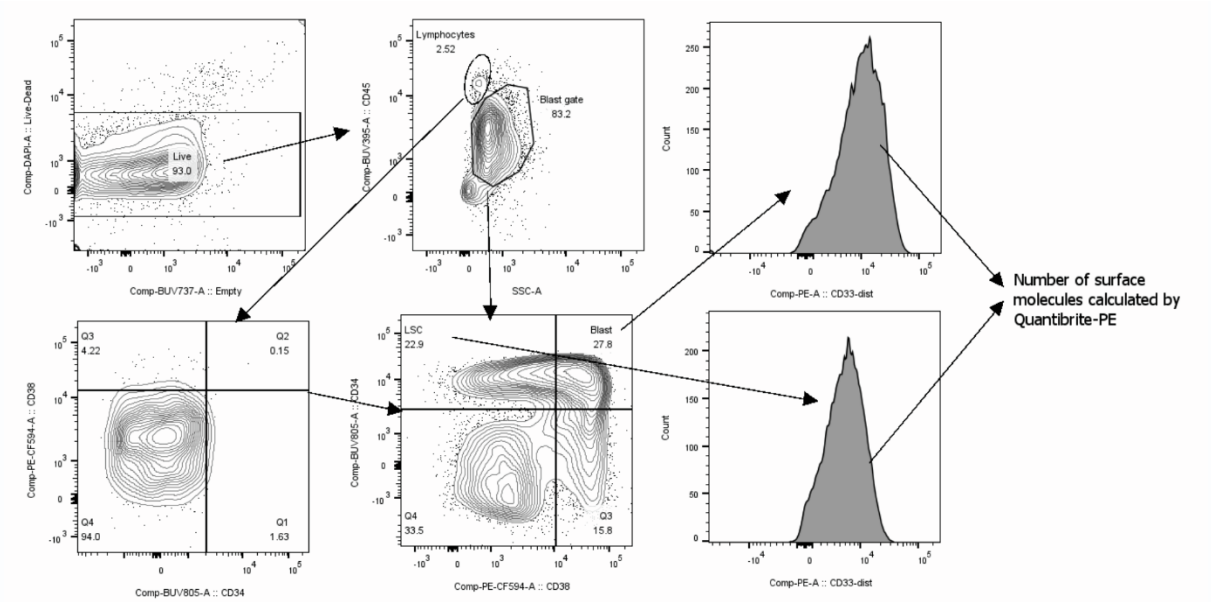

Figure S12.

Gating strategy to identify CD34+ and CD38+ leukemic cells. Representative flow cytometry plot from a bone marrow aspirate of a patient with relapsed/refractory AML showing live cells, and then gating of blasts and lymphocytes based on CD45 vs SSC. Cut-off of CD34 and CD38 based on lymphocyte expression as per Hulspas et al. *Cytometry B Clin Cytom* 2009;76(6):355-364 (PMID: 19575390).